

Diffraction

In the preceding chapter, we focused on some interesting total cross-sections. That is, we were concerned with the behaviour of the (imaginary part of the) scattering amplitudes in the forward direction (i.e. $t = 0$). It is now time to turn our attention to processes which involve the square of the scattering amplitude. Since in the Regge limit the centre-of-mass energy is much larger than the momentum transferred from the incoming particles to any of the outgoing particles such processes must produce a rapidity gap (see Section 1.10) in the final state.

After a brief word regarding elastic scattering at $t = 0$ we continue by looking at processes at large t . Of course we will find a high energy behaviour which is driven by the leading eigenvalue of the BFKL kernel. In addition, we demonstrate that large t is a good way of keeping the dynamics perturbative (recall that the impact factors were the only way to ensure this in the $t = 0$ case) and that the dominant contributions are characterized by the physics of diffusion in the transverse plane. After demonstrating these important points, we go on to discuss the specific example of vector meson production in two-photon collisions, i.e. $\gamma\gamma \rightarrow VV$ where V denotes a vector meson.

The second part of this chapter will be concerned with the physics of diffraction dissociation. In particular, we look in some detail at the particular process of photon dissociation in deep inelastic scattering. By working in the proton (target) rest frame we will be able to discuss the process in a way which is appealing to our physical intuition.

7.1 Elastic scattering at $t = 0$

At $t = 0$ we looked, in the preceding chapter, at the specific example of the forward Compton amplitude, $\gamma p \rightarrow \gamma p$. Of course this

amplitude also gives us the corresponding differential distribution, $d\sigma/dt$, for the elastic processes at $t = 0$ via

$$\left. \frac{d\sigma}{dt} \right|_{t=0} = \frac{|A(s, 0)|^2}{16\pi s^2}. \quad (7.1)$$

A similar process, with a higher rate (than the Compton process), is that of $\gamma p \rightarrow V p$ where V is a vector meson and the photon can be real or virtual. For real photons, there is the possibility of using perturbation theory provided the meson is heavy enough. For virtual photons one can study the production of both light and heavy mesons. As well as acting as a possible probe of the perturbative dynamics, these processes allow important information to be extracted about the physics that determines the γV impact factor, which cannot be computed purely within perturbation theory. There has been much interest in this process and here we merely refer to the original papers by Ryskin (1993), Brodsky *et al.* (1994) and the review by Abramowicz, Frankfurt & Strikman (1995).

7.2 Diffusion in large t elastic scattering

In Chapter 4, we derived an expression for the elastic-scattering amplitude at large t (see Eq.(4.52)). We could now proceed to convolute the universal four-point function of Eq.(4.52) with some appropriate impact factors in order to compute the physical cross-sections. However, we need first to establish the circumstances under which perturbation theory ought to apply. Recall the discussion of Section 5.1, where (for $t = 0$) it was demonstrated that the typical transverse momenta at some point inside the Pomeron are governed by the scales within the impact factors, with a distribution characterized by the diffusion equation, Eq.(5.1). We would now like to make a similar study for the case of non-zero t .

In terms of the energy variable, $y = \ln s/k^2$, the generic scattering amplitude can be written (see Eq.(4.36))

$$\begin{aligned} \frac{\Im A(s, t)}{s} &= \frac{\mathcal{G}}{(2\pi)^4} \int d^2\mathbf{k}_1 d^2\mathbf{k}_2 \frac{F(y, \mathbf{k}_1, \mathbf{k}_2, \mathbf{q})}{\mathbf{k}_2^2 (\mathbf{k}_1 - \mathbf{q})^2} \\ &\times \Phi_A(\mathbf{k}_1, \mathbf{q}) \Phi_B(\mathbf{k}_2, \mathbf{q}), \end{aligned} \quad (7.2)$$

where Φ_A and Φ_B are the impact factors for the Pomeron coupling to the external particles and the universal four-point function is

given by

$$\begin{aligned} \frac{F(y, \mathbf{k}_1, \mathbf{k}_2, \mathbf{q})}{\mathbf{k}_2^2(\mathbf{k}_1 - \mathbf{q})^2} &= \frac{1}{(2\pi)^6} \int d^2\mathbf{b}_1 d^2\mathbf{b}'_1 d^2\mathbf{b}_2 d^2\mathbf{b}'_2 \\ &\times e^{-i[\mathbf{k}_1 \cdot \mathbf{b}_1 + (\mathbf{q} - \mathbf{k}_1) \cdot \mathbf{b}'_1 - \mathbf{k}_2 \cdot \mathbf{b}_2 - (\mathbf{q} - \mathbf{k}_2) \cdot \mathbf{b}'_2]} \\ &\times \int_{-\infty}^{\infty} d\nu \frac{\nu^2}{(\nu^2 + 1/4)^2} e^{\tilde{\alpha}_s \chi_0(\nu)y} \tilde{\phi}_0^\nu(\mathbf{b}_1, \mathbf{b}'_1, \mathbf{0}) \tilde{\phi}_0^{\nu*}(\mathbf{b}_2, \mathbf{b}'_2, \mathbf{0}). \end{aligned} \quad (7.3)$$

This equation has been obtained from Eqs.(4.46) and (4.52) after a change of variables to eliminate the \mathbf{c} -dependence and after taking the (leading) $n = 0$ approximation.

To investigate the internal dynamics of the Pomeron, it is convenient to introduce the functions,

$$\psi_A(y, \mathbf{r}, \mathbf{q}) = \int \frac{d^2\mathbf{k}}{(2\pi)^2} e^{-i\mathbf{k} \cdot \mathbf{r}} d^2\mathbf{k}_1 \frac{F(y, \mathbf{k}_1, \mathbf{k}, \mathbf{q})}{\mathbf{k}^2(\mathbf{k}_1 - \mathbf{q})^2} \Phi_A(\mathbf{k}_1, \mathbf{q}) \quad (7.4)$$

and

$$\psi_B^*(0, \mathbf{r}, \mathbf{q}) = \int d^2\mathbf{k}_2 e^{i\mathbf{k}_2 \cdot \mathbf{r}} \Phi_B(\mathbf{k}_2, \mathbf{q}). \quad (7.5)$$

These two functions can be thought of as impact factors in impact parameter space (\mathbf{r} is the impact parameter conjugate to the internal momentum, \mathbf{k} and can be thought of as the ‘transverse size’ of the Pomeron), i.e.

$$\frac{\Im A(s, t)}{s} = \frac{\mathcal{G}}{(2\pi)^4} \int d^2\mathbf{r} \psi_A(y, \mathbf{r}, \mathbf{q}) \psi_B^*(0, \mathbf{r}, \mathbf{q}). \quad (7.6)$$

Note that all the BFKL dynamics is subsumed into ψ_A but that, as in Eq.(5.2), we are free to partition the energy dependence as we choose. Also note that these ‘impact factors’ have different dimensions (ψ_A has dimensions of an area whilst ψ_B has dimensions of an inverse area). Equation (7.6) is shown graphically in Fig. 7.1.

We now wish to focus on the \mathbf{r} -dependence of ψ_A as y varies. Physically, we are looking to see what are the typical separations of the two gluons which couple into the lower impact factor (since $\mathbf{r} = \mathbf{b}'_2 - \mathbf{b}_2$). We shall show that the largeness of the momentum transfer, $-t = \mathbf{q}^2$, is sufficient to keep this distance small (and hence support the use of perturbation theory) regardless of the size of the external particles.

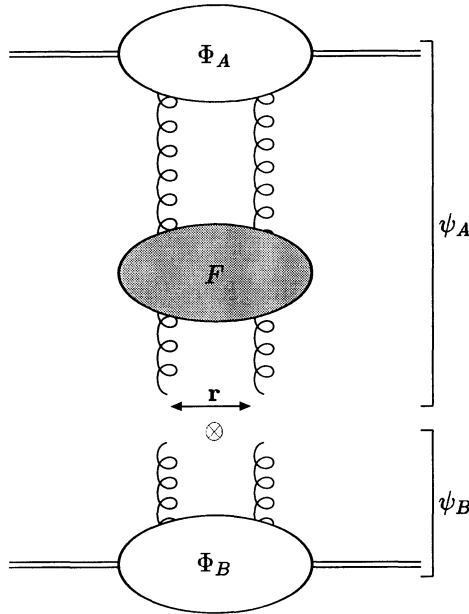


Fig. 7.1. Graphical representation of Eq.(7.6). The convolution represents the integral over the Pomeron transverse size, \mathbf{r} .

Using Eq.(4.49) for $\tilde{\phi}_0^\nu$ we can combine Eqs.(7.3) and (7.4) to write

$$\begin{aligned} \psi_A(\mathbf{y}, \mathbf{r}, \mathbf{q}) &= \frac{1}{(2\pi)^6} \int d^2\mathbf{R} \int d\nu \frac{\nu^2}{(\nu^2 + 1/4)^2} e^{\tilde{\alpha}_s \chi_0(\nu)y} \\ &\times V_\nu(\mathbf{q}, Q) \left[\frac{\mathbf{r}^2}{(\mathbf{R} - \mathbf{r}/2)^2 (\mathbf{R} + \mathbf{r}/2)^2} \right]^{1/2 - i\nu} e^{i\mathbf{q} \cdot (\mathbf{R} - \mathbf{r}/2)}, \end{aligned} \tag{7.7}$$

where the impact factor dependent term is

$$\begin{aligned} V_\nu(\mathbf{q}, Q) &= \int d^2\mathbf{k}_1 d^2\mathbf{b}_1 d^2\mathbf{b}'_1 e^{-i[\mathbf{k}_1 \cdot \mathbf{b}_1 + (\mathbf{q} - \mathbf{k}_1) \cdot \mathbf{b}'_1]} \\ &\times \Phi_A(\mathbf{k}_1, \mathbf{q}) \left[\frac{(\mathbf{b}_1 - \mathbf{b}'_1)^2}{\mathbf{b}_1^2 \mathbf{b}'_1{}^2} \right]^{1/2 + i\nu}. \end{aligned} \tag{7.8}$$

Note that we have changed variables from \mathbf{b}_2 and \mathbf{b}'_2 to

$\mathbf{R} = (\mathbf{b}_2 + \mathbf{b}'_2)/2$ and the \mathbf{k} -integral in Eq.(7.4) gives a delta function which fixes $\mathbf{r} = \mathbf{b}'_2 - \mathbf{b}_2$. Also, we have written explicitly the dependence of V_ν upon the scale Q , which characterizes the size of the particle A .

The fact that the eigenfunctions of the kernel are no longer simple powers of the momentum mean that we must face up to the rather unwieldy nature of these expressions. However, it is possible to perform the two-dimensional \mathbf{R} -integral by introducing a Feynman parameter, x , and using standard integrals (see e.g. Gradshteyn & Ryzhik (1994)). This gives

$$\begin{aligned} \psi_A(y, \mathbf{r}, \mathbf{q}) &= \frac{r}{(2\pi)^5} \int_{-\infty}^{\infty} d\nu \frac{\nu^2}{(\nu^2 + 1/4)^2} e^{\tilde{\alpha}_s \chi_0(\nu)y} V_\nu(\mathbf{q}, Q) \\ &\times \frac{1}{\Gamma^2(1/2 - i\nu)} \int_0^1 \frac{dx e^{-i\mathbf{q}\cdot\mathbf{r}x}}{\sqrt{x(1-x)}} \left(\frac{\mathbf{q}^2}{4}\right)^{-i\nu} K_{2i\nu}(qr\sqrt{x(1-x)}), \end{aligned} \quad (7.9)$$

where $K_{2i\nu}(qr\sqrt{x(1-x)})$ is a modified Bessel function (see, e.g. Abramowitz & Stegun (1972)) and, as usual, non-boldface is used to denote the modulus of the two-vectors.

Subsequent development clearly necessitates that we say something about the impact factor. However, the presence of the $(\mathbf{q}^2)^{-i\nu}$ factor allows us to recognize that a similar factor must be present in V_ν . In particular, we consider the simplest case where the impact factor is pointlike (i.e. has no scale, Q). Thus we take

$$V_\nu(\mathbf{q}, Q) = (\mathbf{q}^2/4)^{-1/2+i\nu}.$$

We can now write

$$\begin{aligned} \psi_A(y, \mathbf{r}, \mathbf{q}) &= \frac{1}{(2\pi)^5} \int d\nu \frac{\nu^2}{(\nu^2 + 1/4)^2} e^{\tilde{\alpha}_s \chi_0(\nu)y} \frac{2r/q}{\Gamma^2(1/2 - i\nu)} \\ &\times \int_0^1 \frac{dx}{\sqrt{x(1-x)}} e^{-i\mathbf{q}\cdot\mathbf{r}x} K_{2i\nu}(qr\sqrt{x(1-x)}). \end{aligned} \quad (7.10)$$

In general, the \mathbf{r} angular integral is non-trivial when performing the convolution with the ψ_B impact factor. However, we are presently interested in the typical values of the modulus of \mathbf{r} within ψ_A . As such we consider the angular integrated quantity

$$\begin{aligned} \bar{\psi}_A(y, r, q) &= \frac{1}{(2\pi)^4} \int d\nu \frac{\nu^2}{(\nu^2 + 1/4)^2} e^{\bar{\alpha}_s \chi_0(\nu)y} \frac{2r/q}{\Gamma^2(1/2 - i\nu)} \\ &\times \int \frac{dx}{\sqrt{x(1-x)}} J_0(qrx) K_{2i\nu}(qr\sqrt{x(1-x)}), \end{aligned} \quad (7.11)$$

where $J_0(qrx)$ is a Bessel function.

For $qr \lesssim 1$ we can use the small argument expansion of the Bessel functions. In which case,

$$\begin{aligned} \bar{\psi}_A(y, r, q) &\approx \frac{1}{(2\pi)^4} \int d\nu \frac{\nu^2}{(\nu^2 + 1/4)^2} e^{\bar{\alpha}_s \chi_0(\nu)y} \int \frac{dx}{\sqrt{x(1-x)}} \\ &\times \left[\frac{[qr/2\sqrt{x(1-x)}]^{2i\nu}}{\Gamma(1 + 2i\nu)} - \frac{[qr/2\sqrt{x(1-x)}]^{-2i\nu}}{\Gamma(1 - 2i\nu)} \right] \\ &\times \frac{2r/q}{\Gamma^2(1/2 - i\nu)} \frac{i\pi}{2\sinh 2\pi\nu}. \end{aligned} \quad (7.12)$$

The x -integral can now be performed and after taking the limit of small ν (which, as usual, will give the dominant contribution for large enough y) it can be shown that

$$\bar{\psi}_A(y, r, q) \approx \frac{1}{\pi^4} \int d\nu \nu e^{\omega_0 y - a^2 \nu^2} \sin\left(\nu \ln \frac{16}{q^2 r^2}\right) \frac{r}{q}, \quad (7.13)$$

where $a^2 = 14\bar{\alpha}_s \zeta(3)$. Performing the ν -integral then yields our final result, i.e.

$$\bar{\psi}_A(y, r, q) \approx \frac{1}{2\pi^4} \frac{\sqrt{\pi r}}{q} \frac{e^{\omega_0 y}}{(a^2 y)^{3/2}} \xi \exp\left(-\frac{\xi^2}{4a^2 y}\right), \quad (7.14)$$

where $\xi \equiv \ln(16/q^2 r^2)$. Notice that $\bar{\psi}_A/r$ is also a solution to the diffusion equation of Section 5.1, i.e. Eq.(5.1).

For $qr \gg 1$, the x -integral is dominated by the end-point regions (close to 0 and 1). We can then approximate Eq.(7.11) by

$$\begin{aligned} \bar{\psi}_A(y, r, q) &\approx \frac{1}{(2\pi)^4} \int d\nu \frac{\nu^2}{(\nu^2 + 1/4)^2} e^{\bar{\alpha}_s \chi_0(\nu)y} \frac{2r/q}{\Gamma^2(1/2 - i\nu)} \\ &\times \int_0^\infty \frac{dx}{\sqrt{x}} K_{2i\nu}(qr\sqrt{x}) [1 + J_0(qr)]. \end{aligned} \quad (7.15)$$

Note that we can concentrate on the $x \rightarrow 0$ end-point (since the $x \rightarrow 1$ contribution is identical) and the upper limit on the

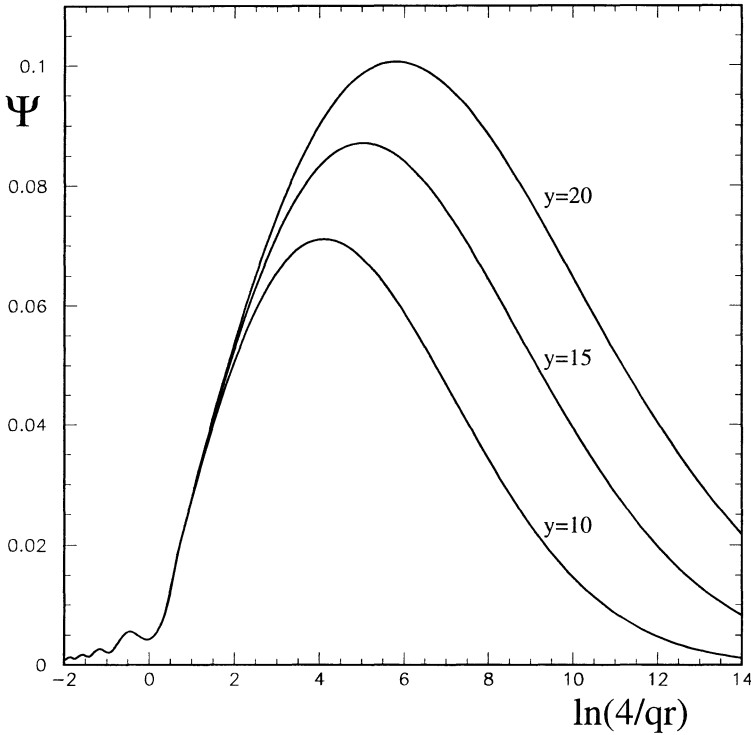


Fig. 7.2. The function Ψ as a function of $\ln(4/qr)$ ($= \xi/2$) at different y values.

x -integral can be approximated by infinity within our approximations. Equation (7.15) can be integrated about the saddle point at $\nu = 0$ to yield

$$\bar{\psi}_A(y, r, q) \approx \frac{1}{(2\pi)^4} \frac{16\sqrt{\pi r}}{q} \frac{e^{\omega_0 y}}{(a^2 y)^{3/2}} \frac{1}{qr} [1 + J_0(qr)]. \quad (7.16)$$

Note that there is no diffusion into (or from) this region.

In Fig. 7.2 we plot the ξ -dependence of

$$\Psi \equiv \bar{\psi}_A \frac{\pi q}{2r} \left[\frac{e^{\omega_0 y}}{(a^2 y)^{3/2}} \right]^{-1},$$

i.e. we have divided out the typical energy dependent factors to allow a clear demonstration of the diffusion properties. It clearly illustrates the dominance of the region $\xi \gtrsim 0$. Notice that for $\xi > 0$

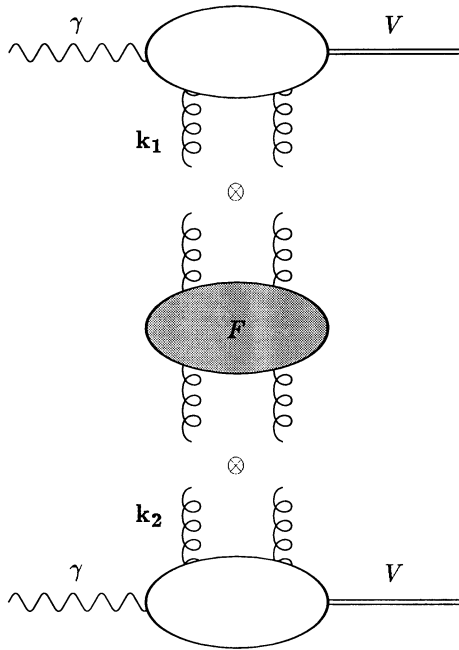


Fig. 7.3. The quasi-elastic scattering process $\gamma\gamma \rightarrow VV$.

there is diffusion, i.e. the width in ξ increases with increasing y , indicating that as the energy increases a larger range of the Pomeron transverse size is important. On the other hand for $\xi < 0$ there is no change in shape as y varies. Indeed, the contribution for $\xi < 0$ is very small. We see that the momentum transfer acts as a dividing scale between the region of diffusion (which is dominant) and the scaling region (where the contribution is small). So, for large enough $-t$ we can be sure that the dominant contribution arises from small values of the Pomeron transverse size for which the QCD coupling is small. In this region we expect perturbation theory to be valid.

To make these features more explicit, let us look at a specific example. Namely, we consider the process shown in Fig. 7.3, i.e. $\gamma\gamma \rightarrow VV$, where V is a vector meson. The incoming photons are assumed to be on shell. A suitable model for the impact factor is

to take

$$\Phi_A(\mathbf{k}_1, \mathbf{q}) = C \left(\frac{1}{m^2 + (\mathbf{k} - \mathbf{q}/2)^2} - \frac{1}{m^2 + \mathbf{q}^2/4} \right), \quad (7.17)$$

where C is a dimensionful constant and depends upon the mass (m) and decay width of the vector meson state. This is something of a toy impact factor, in that it assumes that the quark and antiquark which form the meson carry equal fractions of the photon energy. It can be calculated along the same lines as the impact factor of Eq.(4.44). Nevertheless, it will suffice for the discussion of the general properties that follow.

With this impact factor, the function $V_\nu(\mathbf{q}, m)$ of Eq.(7.8) can be computed (this is not a straightforward calculation and here we quote only the result and refer to Bartels, Forshaw, Lotter & Wüsthoff (1996) for the details). One finds, in the limit of $\mathbf{q}^2 \gg m^2$, that

$$V_\nu(\mathbf{q}, m) \sim \frac{C}{\mathbf{q}^2} \ln \frac{\mathbf{q}^2}{m^2} \left(\frac{\mathbf{q}^2}{4} \right)^{-1/2+i\nu} \quad (7.18)$$

and we do not write explicitly the constant prefactor. Note that, modulo the logarithm, we could have anticipated this form on purely dimensional grounds.

To compute the scattering amplitude, we need to convolute ψ_A with ψ_B , where

$$\begin{aligned} \psi_B^*(0, \mathbf{r}, \mathbf{q}) &= C \int d^2\mathbf{k} e^{i\mathbf{k}\cdot\mathbf{r}} \left(\frac{1}{m^2 + (\mathbf{k} - \mathbf{q}/2)^2} - \frac{1}{m^2 + \mathbf{q}^2/4} \right) \\ &= C 2\pi e^{-i\mathbf{q}\cdot\mathbf{r}/2} \left(K_0(mr) - \frac{2\pi\delta^2(\mathbf{r})}{\mathbf{q}^2/4 + m^2} \right). \end{aligned} \quad (7.19)$$

The delta function term gives zero upon convolution with ψ_A . The factor ψ_B does not spoil the dominance of the contribution from the region $\xi > 0$. As such, the angular part of the \mathbf{r} integral can be approximated by 2π and we can use Eqs.(7.6), (7.14), (7.18) and (7.19) to write (again modulo an overall constant prefactor which is of no interest to us)

$$\begin{aligned} \frac{\Im m A(s, t)}{s} &\sim \frac{C^2}{q^3} \ln \frac{q^2}{m^2} \frac{e^{\omega_0 y}}{(a^2 y)^{3/2}} \\ &\times \int_0^{\sim 1/q} dr r^2 K_0(mr) \xi e^{-\xi^2/(4a^2 y)}. \end{aligned} \quad (7.20)$$

The r -integral can now be done since it is safe to take the small argument expansion of the Bessel function because $m^2 \ll q^2$, i.e. $K_0(mr) \approx \ln(1/mr)$. We integrate over the dominant region of $\xi > 0$, i.e. contributions from $r \gtrsim 1/q$ are heavily suppressed, and find

$$\frac{\Im A(s, t)}{s} \sim \frac{C^2}{q^6} \ln^2 \left(\frac{q^2}{m^2} \right) \frac{e^{\omega_0 y}}{(a^2 y)^{3/2}} \quad (7.21)$$

and hence,

$$\frac{d\sigma}{dt} \sim \frac{C^4}{t^6} \ln^4 \left(\frac{q^2}{m^2} \right) \frac{e^{2\omega_0 y}}{(a^2 y)^3}. \quad (7.22)$$

A large- t elastic-scattering process that is typically more accessible to experiment is that of parton-parton elastic scattering. This has been investigated in hadron-hadron collisions (Abe *et al.* (1995), Abachi *et al.* (1994)) and in photon-hadron collisions (Derrick *et al.* (1996b)). In such processes a pair of partons (one from each 'hadron') scatter elastically off each other via the exchange of a Pomeron to produce a pair of jets which are separated by a large gap in rapidity. To lowest order, the transverse momentum of the jets produced by the scattered partons is equal to (the modulus of) the momentum transfer, $|t|$. We have chosen not to focus on these processes owing to the complications discussed at the end of Section 4.5 which arise whenever the Pomeron couples to a single parton.

So we have demonstrated that elastic scattering at large enough $-t$ can be calculated in perturbative QCD,[†] at least in those cases where the dominant contribution arises due to the exchange of a pair of (interacting) reggeized gluons. In particular, one can envisage elastic scattering processes where the dominant contribution is *not* due to Pomeron exchange. For example proton-proton elastic scattering at high- t is dominated by (at the Born level) three-gluon exchange. This is because if one views the scattering as occurring between the three constituent quarks in each proton then it is preferential to deflect each quark through the same angle. At lowest order, this then requires three gluons to be exchanged (each

[†] Of course the impact factors ($\Phi_{A,B}$) are generally not calculable in perturbation theory. What we have shown is that this physics essentially factorizes and the exchange dynamics is dominated by the perturbative contribution.

coupling to three constituent quarks per proton). So although one pays the price of an additional power of α_s , this is more than compensated by the need to share the kick delivered by the momentum transfer equally between the constituents (Landshoff (1974)).

7.3 Diffraction dissociation and Pomeron substructure

Our focus in this section will be on the dissociation of a high Q^2 photon in $\gamma^*p \rightarrow Xp$ (where X denotes the diffracted system). This process is of particular interest since one can think of performing *deep inelastic scattering off a Pomeron target*. The possibility of unravelling the partonic substructure of the Pomeron thus presents itself. We shall have more to say on this interpretation a little later.

However, in order to prepare the ground for our discussion of the photon dissociation process we wish first to return to the inclusive deep inelastic process and its interpretation in the proton rest frame. This way of looking at the inclusive process will better equip us for our study of that subset of events containing a fast-forward proton (i.e. photon dissociation).

7.3.1 The proton rest frame picture

Recall the impact factors for deep inelastic scattering, Eq.(A.6.15) and Eq.(A.6.16). Using the identities

$$\int \frac{d^2\mathbf{l}}{(\mathbf{l}^2 + \epsilon^2)((1 - \mathbf{k})^2 + \epsilon^2)} = \int d^2\mathbf{r} e^{i\mathbf{k}\cdot\mathbf{r}} K_0^2(\epsilon r) \tag{7.23}$$

and

$$\int \frac{d^2\mathbf{l}}{(\mathbf{l}^2 + \epsilon^2)^2} = \int d^2\mathbf{r} K_0^2(\epsilon r), \tag{7.24}$$

we can re-write the longitudinal impact factor as follows (replacing ρ in Eq.(A.6.15) by z),

$$\begin{aligned} \Phi_L(\mathbf{k}) &= 32\alpha_s \sum_{q=1}^{n_f} e_q^2 \int_0^1 dz \int d^2\mathbf{r} (1 - e^{i\mathbf{k}\cdot\mathbf{r}}) \\ &\quad \times Q^2 z^2 (1 - z)^2 K_0^2(\epsilon r), \end{aligned} \tag{7.25}$$

where $\epsilon^2 = z(1 - z)Q^2$.

Thus, the cross-section for the scattering of longitudinal photons is (see Eqs.(6.3) and (6.5))

$$\sigma_L(x, Q^2) = \int dz d^2\mathbf{r} |\Psi_L(z, r)|^2 \sigma(x, r), \quad (7.26)$$

where

$$|\Psi_L(z, r)|^2 = \frac{6}{\pi^2} \alpha \sum_{q=1}^{n_f} e_q^2 Q^2 z^2 (1-z)^2 K_0^2(\epsilon r) \quad (7.27)$$

and

$$\sigma(x, r) = \frac{4\pi\alpha_s}{3} \int \frac{d^2\mathbf{k}}{\mathbf{k}^4} \mathcal{F}(x, \mathbf{k}) (1 - e^{i\mathbf{k}\cdot\mathbf{r}}). \quad (7.28)$$

Similarly the cross-section for the scattering of transverse photons is given by

$$\sigma_T(x, Q^2) = \int dz d^2\mathbf{r} |\Psi_T(z, r)|^2 \sigma(x, r), \quad (7.29)$$

where

$$|\Psi_T(z, r)|^2 = \frac{3}{2\pi^2} \alpha \sum_{q=1}^{n_f} e_q^2 [z^2 + (1-z)^2] \epsilon^2 K_1^2(\epsilon r). \quad (7.30)$$

By writing the cross-sections in such a way we have made explicit a result which has a very clear physical interpretation. In the proton rest-frame, and for low enough values of x , the photon produces the $q\bar{q}$ pair a long distance ‘down stream’ of the proton (as indicated in Fig. 7.4). Some (long) time later, this pair then scatters coherently off the proton. The typical time-scale of the interaction (of the $q\bar{q}$ pair) with the proton is very short (relative to the formation time of the pair) and as such we can consider *the transverse size of the pair to be fixed over the time of the interaction*. Consequently, we can interpret $\sigma(x, r)$ as the cross-section for the scattering of a $q\bar{q}$ pair of transverse size r off the target proton and $\Psi(z, r)$ as the wavefunction describing the formation of a $q\bar{q}$ pair where z and $1-z$ are the fractions of the photon energy carried by the quark and antiquark. We shall shortly justify the precise normalizations of the wavefunctions. Let us first make this physical picture a little more explicit.

We work in terms of light-cone variables, i.e. the photon momentum is written, $q = (q^+, q^-, \mathbf{0})$ where

$$q^+ = q_0 + q_3 \gg q^- = q_0 - q_3 = -Q^2/q^+$$

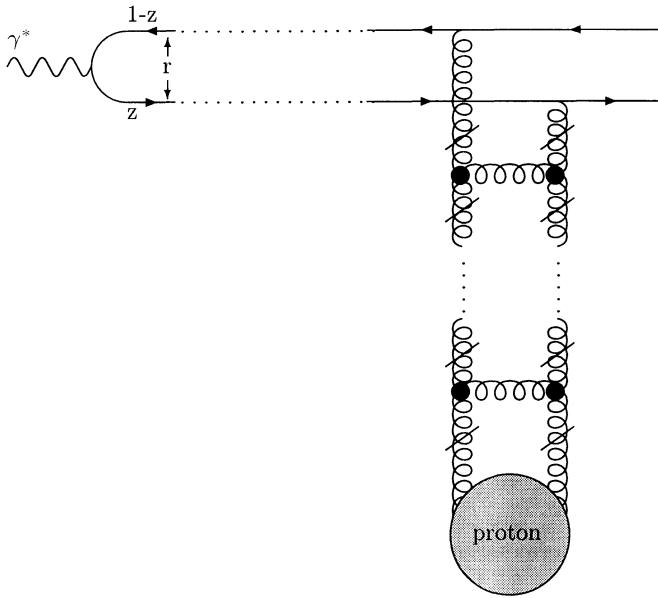


Fig. 7.4. The formation of a $q\text{-}\bar{q}$ pair from a virtual photon, followed a long time (on the scale of hadronic interactions) later by the scattering of the pair off a proton via the exchange of a Pomeron (which, for small enough r , is the ladder of reggeized gluons shown).

(q_μ are the components of the photon four-momentum vector). The quark carries momentum,

$$l_q = \left(zq^+, \frac{\mathbf{l}^2}{zq^+}, \mathbf{l} \right),$$

and the antiquark momentum is obtained by replacing $z \rightarrow 1 - z$ and $\mathbf{l} \rightarrow -\mathbf{l}$. Putting the quarks on shell, we see that the energy imbalance, ΔE , between the photon and the $q\text{-}\bar{q}$ pair, is given by

$$\begin{aligned} \Delta E &= (l_q^+ + l_{\bar{q}}^- + l_{\bar{q}}^+ + l_q^- - q^+ - q^-)/2 \\ &= \frac{1}{2q^+} \left(Q^2 + \frac{\mathbf{l}^2}{z(1-z)} \right). \end{aligned}$$

Now since $2p \cdot q = Q^2/x$ and $p = (M_p, M_p, 0)$ (M_p is the proton

mass) it follows that

$$q^+ \approx \frac{Q^2}{M_p x}$$

and hence

$$\Delta E \approx \left(Q^2 + \frac{\mathbf{l}^2}{z(1-z)} \right) \frac{M_p x}{2Q^2}.$$

Provided $\mathbf{l}^2/(z(1-z)) \lesssim Q^2$ (which will always be the case in our subsequent considerations), it then follows, from the uncertainty principle, that the $q-\bar{q}$ pair propagate typical longitudinal distances $\sim 1/(M_p x)$ before interacting with the proton. Since we are in the low- x regime, these distances can be huge on the scale of the proton radius. Put another way, the lifetime of the $q-\bar{q}$ fluctuations of the virtual photon is huge in comparison with the typical time over which the pair interact with the target; as such we can consider the transverse size of the pair to be frozen over the time of interaction.

It is now time to make the identification of the wavefunction and cross-section more precise (in particular to determine their normalizations). Our strategy is first to establish the normalization of the transversely polarized photon wavefunction. We will then be able to infer the normalization of the cross-section $\sigma(x, r)$ and (since this cross-section does not depend upon the photon polarization) this will be sufficient to fix the normalization of the longitudinal photon wavefunction.

To lowest order, the virtual photon can either interact as a photon or via its fluctuation into a fermion-antifermion pair, i.e. denoting the physical state by $|\gamma_{\text{phys}}\rangle$ we have

$$|\gamma_{\text{phys}}\rangle = \sqrt{Z_3} |\gamma_B\rangle + c |f\bar{f}\rangle. \quad (7.31)$$

Z_3 is the photon wavefunction renormalization constant, $|\gamma_B\rangle$ denotes the bare photon state and c is some coefficient (to be determined) which determines the probability that the photon is to be found in the $f-\bar{f}$ state (f labels the fermion type). Note that since we are including the possibility that the photon fluctuates into the $f-\bar{f}$ pair (i.e. $c^2 = \mathcal{O}(\alpha)$) we must work to the same order in the bare photon renormalization (i.e. $Z_3^2 = 1 + \mathcal{O}(\alpha)$).

Since we are interested in the (dominant) strong interactions of the photon with the target it follows that we are only interested

in the $q\bar{q}$ fluctuations of the virtual photon. We need to compute the coefficient, c , in this case. Working with properly normalized states, i.e. $\langle\gamma|\gamma\rangle = \langle\gamma_B|\gamma_B\rangle = \langle q\bar{q}|q\bar{q}\rangle = 1$ it follows that

$$c^2 = 1 - Z_3. \tag{7.32}$$

For transversely polarized photons, Z_3 is ultra-violet divergent. Imposing an ultra-violet cut-off Λ on the transverse momentum of the $q\bar{q}$ pair we can write (keeping only the leading logarithm in the ultra-violet cut-off)

$$c^2 \approx \frac{\alpha}{\pi} \sum_{q=1}^{n_f} e_q^2 \ln \frac{\Lambda^2}{Q^2}. \tag{7.33}$$

(and we have summed over the three colours of quark). Since

$$\int dz d^2\mathbf{r} |\Psi_T(z, r)|^2 = c^2, \tag{7.34}$$

we have therefore fixed the normalization of the wavefunction for transverse photons. It is easy to check that this is consistent with the definitions given in Eqs.(7.26)–(7.30).

It is important to realize that Eqs.(7.26) and (7.29) are perfectly general (i.e. they are valid beyond perturbation theory). This is because they are determined purely by the space-time structure of the process. For small size $q\bar{q}$ pairs, we can compute the wavefunction, $\Psi_{L,T}$, and the radiative corrections to $\sigma(x, r)$ which determine the QCD scaling violations. For larger sizes, perturbation theory is useless. For example, in pion–proton scattering Eq.(7.26) can be used to determine the scattering of the lowest Fock state ($q\bar{q}$) component of the pion off the proton. In this case the pion wavefunction, $\Psi_\pi(z, r)$, is normalized to unity.

It is correct to say that by working in this representation we have succeeded in diagonalizing the scattering matrix. To see this consider the elastic-scattering amplitude, $A(s, 0)$. In terms of the T -matrix elements

$$\Im m A(s, 0) = \langle\gamma|T|\gamma\rangle. \tag{7.35}$$

We can expand the photon state as a sum over the interaction eigenstates, $|\psi_k\rangle$ i.e.

$$|\gamma\rangle = \sum_k c_k |\psi_k\rangle, \tag{7.36}$$

where $\sum_k |c_k|^2 = 1$. That the $|\psi_k\rangle$ are eigenstates of the interaction means that

$$T|\psi_k\rangle = p_k|\psi_k\rangle, \quad (7.37)$$

where p_k is the probability that eigenstate k scatters off the target. So the imaginary part of the elastic scattering amplitude can be written

$$\Im A(s, 0) = \sum_k |c_k|^2 p_k. \quad (7.38)$$

Comparing with Eqs.(7.26) and (7.29) we identify the interaction eigenstates with the set of parton states at fixed impact parameters and energy fractions (i.e. k labels the (r, z) of the interaction). p_k/s is then to be identified with the cross-section for scattering the interaction eigenstate off the target, i.e. $\sigma(r)$. Note that here we have considered the special case of elastic scattering, but it is clear that there is also the possibility of producing new states (which carry the quantum numbers of the photon). This is the process of diffraction dissociation and it is clear that the interaction eigenstates we have just been discussing are more generally the eigenstates of diffraction (of which elastic scattering is a special case). The identification of the diffraction eigenstates with the frozen partonic configurations was first made by Miettinen & Pumplin (1978).

Let us now investigate the physics of the elastic scattering amplitude. For small enough r , $\sigma(x, r) \sim r^2$, modulo scaling violations (this can be seen after expanding the exponential in Eq.(7.28) and performing the angular integral). Thus, small size pairs scatter with a cross-section which vanishes as the square of their separation. For large enough r , confinement dictates that the cross-section should saturate at a constant value of the order of a typical hadronic size. Both of these properties are necessary in order to understand the scaling of the deep inelastic structure functions (modulo the scaling violations induced by QCD corrections). Let us see why this is so.

We need to examine the Q^2 -behaviour of the longitudinal and transverse cross-sections (Eqs.(7.26) and (7.29)) arising from the contributions from large size and small size $q-\bar{q}$ pairs. We expect the contributions from small size pairs to be calculable in perturbation theory whereas those from large size pairs are expected to be dominated by non-perturbative effects.

The modified Bessel functions $K_i(\epsilon r)$ in Eqs.(7.27) and (7.30) are exponentially suppressed for $\epsilon r \gg 1$. In order to extract the Q^2 -behaviour it suffices to replace $K_0(\epsilon r)$ by $c_0\Theta(1 - \epsilon r)$, i.e. a constant value, c_0 , for $\epsilon r < 1$ and zero otherwise[†] and $K_1(\epsilon r)$ by $c_1\Theta(1 - \epsilon r)/\epsilon r$.

Consider first the contribution to the cross-section which arises from large size pairs, i.e. $r \gtrsim R \gg 1/Q$ ($R \sim 1$ fm). The requirement $\epsilon r < 1$ means that the z -integration is restricted to regions near the end-points, i.e. $z \lesssim 1/Q^2 R^2$ or $(1 - z) \lesssim 1/Q^2 R^2$. Thus the z -integrations give for the squared wavefunctions, $|\Psi_L(z, r)|^2$ and $|\Psi_T(z, r)|^2$,

$$\int_{\epsilon < 1/R} Q^2 z^2 (1 - z)^2 dz \sim \frac{1}{Q^4 R^6},$$

for the longitudinal cross-section and

$$\int_{\epsilon < 1/R} (z^2 + (1 - z)^2) \frac{dz}{R^2} \sim \frac{1}{Q^2 R^4},$$

for the transverse cross-section. The integration over \mathbf{r} gives (from dimensional analysis)

$$\int_R^\infty d^2\mathbf{r} \sigma(x, r) \sim R^2.$$

Thus the transverse cross-section has a large size pair contribution which scales, i.e. it is proportional to $1/Q^2$, whereas the longitudinal cross-section has a large size pair contribution which is suppressed by a further factor of $1/Q^2$.

Now consider the contribution from small size pairs, i.e. $r \lesssim 1/Q$. In this case the z integration is not restricted to the end-points; $z \sim \frac{1}{2}$ and the quark-antiquark pair share the photon energy roughly equally. The contributions from the z -integrations for the longitudinal and transverse cross-sections are both proportional to Q^2 . If the scattering cross-section, $\sigma(x, r)$, is calculated in leading order in perturbation theory (i.e. two-gluon exchange rather than the complete Pomeron ladder shown in Fig. 7.4) then on dimensional grounds we have for the integration over \mathbf{r}

$$\int_0^{1/Q} d^2\mathbf{r} \sigma(x, r) \sim \frac{1}{Q^4},$$

[†] As $r \rightarrow 0$ the function $K_0(\epsilon r)$ behaves like $\log r$. However, this is an integrable singularity and does not affect the validity of this approximation.

so that both the longitudinal and transverse cross-sections scale. Inclusion of the complete ladder (QCD Pomeron) in the calculation of $\sigma(x, r)$ leads to the scaling violations discussed in the preceding chapter.

An alternative way of seeing these same results is to use the fact that, from purely dimensional grounds, we can write

$$\int d^2\mathbf{r} \sigma(r) K_i^2(\epsilon r) \propto \frac{1}{\epsilon^4}. \quad (7.39)$$

This is kept finite since $\epsilon^2 \sim m_q^2$ as $z \rightarrow 0, 1$. Here the quark mass, m_q , acts as the confining scale. So,

$$\sigma_T \sim \int dz \frac{z^2 + (1-z)^2}{\epsilon^2}$$

and

$$\sigma_L \sim \int dz \frac{Q^2 [z(1-z)]^2}{\epsilon^4}.$$

It is clear that the end-point contribution to the z -integral leads to the $1/Q^2$ behaviour of σ_T and the m_q^2/Q^4 behaviour of σ_L . Also, the $z \sim \frac{1}{2}$ contributions clearly yield the $1/Q^2$ behaviour for both longitudinal and transverse cross-sections.

Thus, we have regained the property of Bjorken scaling (neglecting the QCD corrections contained in $\sigma(x, r)$). However, we have gained a little more insight into the final state morphology of low- x deep inelastic events. There are large contributions to the cross-section for scattering of transverse photons from the so-called **aligned jet** configurations (where one parton carries all the photon energy). The small-size configurations also generate a scaling contribution and are associated with the more democratic final state in which the quark and antiquark share the photon energy. The scaling violations to the structure function are also calculable in perturbation theory; only the small size fluctuations evolve in Q^2 . Furthermore, since the longitudinal cross-section is determined by small size fluctuations (the large size fluctuations being suppressed by an extra power of $1/Q^2$) we are able to write $F_L(x, Q^2)$ directly in terms of the parton densities evaluated at the scale, Q^2 . For the transverse cross-section the scaling non-perturbative part arising from large size fluctuations must be obtained from experiment at some fixed Q^2 , whereas the Q^2 -evolution can be calculated perturbatively.

7.3.2 *Introduction to photon dissociation*

We have spent most of this book talking about elastic scattering and, through the optical theorem, total cross-sections. In the preceding subsection we highlighted the fact that the existence of elastic scattering naturally suggests the possibility of diffraction dissociation. A beam of hadrons scattered off some target will typically be either absorbed (perhaps leading to the excitation of the target or emission of some final state particles), scattered elastically or diffracted. What is the physical picture which underpins the connection between the total cross-section, elastic scattering and diffraction scattering? The answer, not surprisingly, lies in an analogy with the physics of diffraction in wave optics. Before discussing the special case of photon dissociation, we wish to spend some time making clear the connection between these apparently such different processes.

Consider a broad beam of plane polarized light, incident on some small piece of polaroid (the target). If the light is polarized at some non-zero angle (relative to the axis of the polaroid) then the component that is polarized parallel to the axis of the polaroid will pass through without scattering, i.e. for this component it is as though the polaroid were absent. The other component, which has its axis of polarization perpendicular to the axis of the polaroid, has a small section of its wavefront which is totally absorbed on passing the polaroid, so that the wavefront is partitioned into two wavefronts which pass either side of the polaroid and interfere with each other producing a diffraction pattern. This diffraction pattern is detected (over and above the constant background from the unscattered component) some distance behind the polaroid. Since the diffracted wave is polarized normal to the axis of the polaroid it necessarily contains a component which is polarized parallel to the (polarization of the) incoming wave and also a component which is polarized perpendicular to the incoming wave.

What has this to do with, for example, scattering a beam of hadrons off some target (e.g. another hadron or a nucleus)? The absorption of the light beam in the polaroid is analogous to the inelastic scattering of the hadron on the target (e.g. producing an excited nuclear state or some multi-particle final state). The diffraction of the incoming wave into the component which car-

ries the same polarization is analogous to the elastic scattering of the beam particle. Finally, we saw that diffraction can lead to the production of a new state (carrying polarization distinct from the incoming beam); this, too, should have an analogy in particle physics: this is what we call diffraction dissociation. New states can be ‘diffracted into existence’ by the interaction with the target. We say that *the diffractive processes are the shadow of the inelastic processes.*

More discussion of the physical picture can be found in the paper by Good & Walker (1960), where beam diffraction was first considered. Let us merely note that in order to open up the diffractive channel, it is important to have energy degeneracies (up to some approximation). In the optical case discussed above the two polarization states were degenerate in energy. In the particle physics case the effective degeneracy is achieved by working at high centre-of-mass energies (so that all masses are small relative to the centre-of-mass energy and the proton does not dissociate). This is why diffraction is characterized by processes which involve large gaps in rapidity.

We are now able to commence our study of the rapidity gap events in deep inelastic scattering. We will start by looking at the simplest diffracted system, namely, the one in which the photon dissociates into a single $q-\bar{q}$ pair, which is separated from the fast moving final-state proton by a large gap in rapidity. A typical contribution to the amplitude is shown in Fig. 7.5. We will work in the so-called Born approximation, i.e. the exchange is modelled by the exchange of two gluons (the BFKL corrections will not alter our essential conclusions). In this case, the cross-section for scattering the $q-\bar{q}$ colour dipole off the proton is only a function of the dipole size, r . Notice that the momentum transfer t is no longer zero; in fact simple kinematics allows us to show that, for $M_p^2 \ll Q^2, M_X^2 \ll W^2$,

$$-t_{\min} = (M_X^2 + Q^2)^2 \frac{M_p^2}{W^4}, \quad (7.40)$$

where M_X is the invariant mass of the diffractive system (in this case the $q-\bar{q}$ pair) and W is the $\gamma-p$ centre-of-mass energy. Clearly, for large enough W , t_{\min} is very small (on the scale of the hadron mass). Since we insist that the proton remain intact, it follows

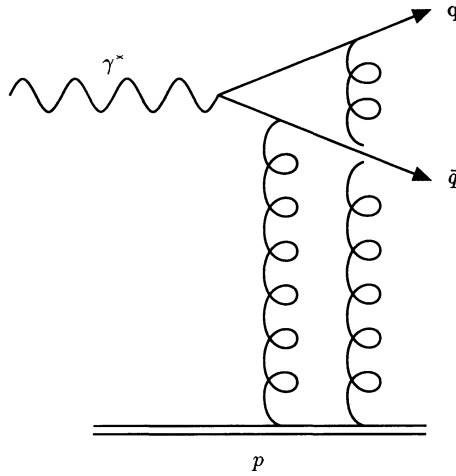


Fig. 7.5. One of the contributions to the amplitude for the process $\gamma p \rightarrow q\bar{q}p$.

that $-t \sim -t_{\min}$ since larger values of $-t$ are suppressed by some hadronic form factor (i.e. it is unlikely that the proton will remain intact after undergoing a large t interaction). Consequently, we will assume that $t = 0$ is a good approximation.

Due to the space-time picture which was discussed in the preceding subsection, we are able to think of the $q\text{-}\bar{q}$ pair in terms of eigenstates of the diffraction scattering matrix. Consequently, we can write the amplitude as a convolution of the squared amplitude for the $\gamma \rightarrow q\bar{q}$ formation with the square of the dipole cross-section, i.e.

$$\left. \frac{d\sigma_{T,L}^D}{dt} \right|_{t=0} = \int_0^1 dz \int d^2\mathbf{r} |\psi_{T,L}(z, \mathbf{r})|^2 \frac{\sigma(r)^2}{16\pi}. \tag{7.41}$$

Let us start by proving this result. In the notation of the preceding subsection, we can write

$$\left. \frac{d\sigma^D}{dt} \right|_{t=0} = \frac{\sum_k |\langle \gamma | T | \psi_k \rangle|^2}{16\pi s^2} - \left. \frac{d\sigma^{el}}{dt} \right|_{t=0} \tag{7.42}$$

and we have subtracted off the elastic cross-section in order to

define the diffractive rate. Substituting for the elastic rate gives

$$\left. \frac{d\sigma^D}{dt} \right|_{t=0} = \frac{1}{16\pi s^2} \left(\sum_k |\langle \gamma | T | \psi_k \rangle|^2 - |\langle \gamma | T | \gamma \rangle|^2 \right). \quad (7.43)$$

Decomposing the photon into the sum over scattering eigenstates gives

$$\left. \frac{d\sigma^D}{dt} \right|_{t=0} = \frac{1}{16\pi s^2} \left[\sum_k |c_k|^2 p_k^2 - \left(\sum_k |c_k|^2 p_k \right)^2 \right]. \quad (7.44)$$

Identifying the label k with the pair size and longitudinal momentum fraction we thus arrive at our final result:

$$\left. \frac{d\sigma^D}{dt} \right|_{t=0} = \frac{\langle \sigma^2 \rangle - \langle \sigma \rangle^2}{16\pi}, \quad (7.45)$$

where we have written the cross-section averaged over the photon wavefunction in a compact form, i.e.

$$\langle \sigma^n \rangle \equiv \int dz d^2 \mathbf{r} |\psi(z, \mathbf{r})|^2 \sigma(r)^n. \quad (7.46)$$

Neglecting the second term (since it is suppressed by a power of α for photon scattering) we thus establish the validity of Eq.(7.41).

The essential difference in comparison with the inclusive case is the presence of the extra factor of $\sigma(r)$. By arguments along the lines of those of the preceding subsection, we now see that diffractive $q-\bar{q}$ production from transverse photons is dominated by large sizes of the $q-\bar{q}$ pair, i.e. the aligned jet configurations (Bjorken (1994)). Note also that the leading behaviour is $\sim 1/Q^2$ (i.e. the same order in Q^2 as the inclusive cross-section). Contrast this with the inclusive cross-section, where the leading (scaling) contribution samples both large and small size pairs. In the diffractive case, the extra factor of $\sigma(r)$ leads to the suppression of the short-distance contribution by a power of $1/Q^2$. For the production from longitudinal photons, we have the result that the short and long distance contributions mix. However, both contributions are suppressed by a power of Q^2 relative to the rate for production from transverse photons.

Note that, in those cases where the large size configurations dominate, it is no longer a good approximation to neglect the quark mass contributions (this is because $\epsilon^2 \sim m_q^2$). Moreover,

for the large size configurations we have no right to use perturbation theory and must (in the absence of any fundamental theory of the non-perturbative regime) rely on a more phenomenological approach. *Despite the fact that the photon has a large virtuality, we have shown that the dominant contribution to the photon dissociation process is of non-perturbative origin.*

Even so, we can go a little further. We can derive an approximate expression for the dependence of the cross-section on the diffracted mass, M_X . If the quark has four-momentum, l_q^μ , where

$$l_q^\mu = (E_q, zp_\gamma, \mathbf{l}),$$

then $l_q^2 = m_q^2$ fixes

$$E_q \approx zp_\gamma + \frac{\mathbf{l}^2 + m_q^2}{2zp_\gamma}$$

in terms of the photon momentum, p_γ . The antiquark four-momentum is once again obtained by replacing $z \rightarrow 1 - z$ and $\mathbf{l} \rightarrow -\mathbf{l}$. The diffracted mass is defined to be the invariant mass of the diffracted system, i.e.

$$M_X^2 \equiv (l_q + l_{\bar{q}})^2 \approx \frac{\mathbf{l}^2 + m_q^2}{z(1 - z)}. \tag{7.47}$$

For the non-perturbative (large size) configurations (which dominate the diffractive rate), the z -integral is dominated by the regions of z close to 0 or 1. From the z near zero region we have,

$$M_X^2 \approx \frac{m_q^2}{z}$$

(since the large size pairs have $\mathbf{l}^2 \sim 0$). Hence we can undo the z -integral and write

$$\frac{d\sigma_T^D}{dt dM_X^2} \sim \frac{m_q^2}{M_X^4} \int d^2\mathbf{r} |\Psi_T(z, r)|^2 \sigma(r)^2. \tag{7.48}$$

As in Eq.(7.39) we see that (from dimensional analysis)

$$\int d^2\mathbf{r} \sigma(r)^2 \epsilon^2 K_i^2(\epsilon r) \propto \frac{1}{\epsilon^4}$$

and, since

$$\begin{aligned} \epsilon^2 &= Q^2 z(1 - z) + m_q^2 \\ &\approx m_q^2 \left(1 + \frac{Q^2}{M_X^2} \right), \end{aligned} \tag{7.49}$$

we have

$$\frac{d\sigma_T^D}{dt dM_X^2} \sim \frac{1}{m_q^2} \frac{1}{(Q^2 + M_X^2)^2}. \quad (7.50)$$

The contribution from the region $z \sim 1$ of course yields the same form. This expression will be a good approximation provided $M_X^2 \gtrsim Q^2 \gg m_q^2$ since for small M_X^2 we can no longer assume that the dominant contribution arises from the end points of the z -integral.

The rate for production of large diffracted masses falls away as $\sim 1/M_X^4$ at large M_X^2 . The origin of this strong decrease can be traced back to the fact that the $q-\bar{q}$ pair scatters directly off the target. It is also possible to radiate additional gluons off the original $q-\bar{q}$ pair and then scatter the resulting multi-parton configuration (frozen in impact parameter) off the target. Of course the radiation of more partons occurs at the price of additional powers in the strong coupling. However, the spin-1 nature of the gluon ensures a weaker decay at large M_X^2 . In fact one expects a $\sim 1/M_X^2$ behaviour. We do not pursue these details at this stage. In the next chapter we will consider the higher Fock components of the photon wavefunction.

7.3.3 The Pomeron structure function

In a frame in which the proton is fast-moving, it is tempting to think of the photon as probing the structure of a Pomeron which has been offered up as an effective target by the proton. The picture (shown in Fig. 7.6) suggests the following form for the diffractive cross-section:

$$\frac{d\sigma_T^D}{dt dx_P} = \frac{4\pi^2\alpha}{Q^2} f(x_P) F_T^P(\beta, Q^2), \quad (7.51)$$

where x_P is the fraction of the incoming proton energy which is carried away by the Pomeron and β is the fraction of the Pomeron momentum carried by the struck quark. The Bjorken- x ($= Q^2/2p \cdot q$) is therefore the product βx_P .

$F_T^P(\beta, Q^2)$ is the structure function of the Pomeron for scattering off transverse photons (it scales in the absence of QCD corrections) and $f(x_P)$ is a factor which determines the Pomeron flux. For simplicity we ignore any t -dependence on the right hand

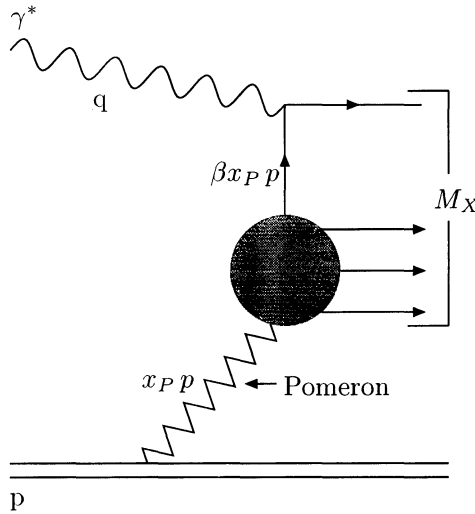


Fig. 7.6. Diffractive photon dissociation process in which a Pomeron is ‘emitted’ by the proton with fraction, x_P , of the proton momentum, p . The Pomeron is probed by a virtual photon of momentum q , which strikes a quark inside the Pomeron that carries a fraction β of the Pomeron momentum. M_X is the invariant mass of the Pomeron–photon system.

side (i.e. we are interested only in the behaviour near $t = 0$). Since $(x_P p + q)^2 = M_X^2$ and $W^2 = (p + q)^2$ (p is the proton four-momentum) we have

$$x_P = \frac{Q^2 + M_X^2}{Q^2 + W^2}, \tag{7.52}$$

and

$$\beta = \frac{x}{x_P} = \frac{Q^2}{2x_P p \cdot q} = \frac{Q^2}{Q^2 + M_X^2}. \tag{7.53}$$

In terms of these variables, we can re-write the diffractive cross-section for $q\bar{q}$ production (see Eq.(7.50)) as

$$\frac{d\sigma_T^D}{dx_P} \sim \frac{\beta}{x_P} \frac{1}{Q^2} \tag{7.54}$$

and hence

$$F_T^P(\beta, Q^2) \sim \beta,$$

$$f(x_P) \sim \frac{1}{x_P}. \quad (7.55)$$

So the concept of the Pomeron structure function makes sense, at least in the approximation that the diffracted system is a pure $q\bar{q}$ pair of not too small invariant mass.

Note that for $M_X^2 \leq 4m_q^2$ the cross-section must vanish (M_X must be larger than the mass of the quark plus antiquark). For $m_q^2 \ll Q^2$ this means that $\beta \approx 1$. We can crudely account for this effect by taking a Pomeron structure function of

$$F_T^P(\beta, Q^2) \sim \beta(1 - \beta). \quad (7.56)$$

This modification is consistent with Eq.(7.55) since it corresponds to multiplication by the factor $M_X^2/(Q^2 + M_X^2)$ which is ~ 1 in the region we are considering. Note that in reality the suppression as $M_X^2 \rightarrow 4m_q^2$ is faster than any power of $1 - \beta$. To see this, notice that $M_X^2 \rightarrow 4m_q^2$ corresponds to $z \rightarrow \frac{1}{2}$ and $l^2 \rightarrow 0$ (i.e. $r \gg 1/Q$). This is the region where the argument of the Bessel function is large and leads to an exponential suppression.

Processes which probe the structure of the Pomeron (at $t = 0$) are termed **hard-diffractive**. The two main types of process we have in mind are deep inelastic diffraction (discussed above) and those processes where hadronic jets are produced in the diffracted system, as in Fig. 7.7. Of course these are the analogous processes to their non-diffractive counterparts, which are used to constrain hadronic parton densities.

If the concept of a Pomeron structure function is to be useful it should be *universal*. That is to say there should exist hard-diffractive processes which are driven by a common set of Pomeron parton distribution functions. This property of universality is certainly not an obvious consequence of QCD. In those hard-diffractive processes where soft physics dominates and the soft Pomeron (which is, so far, well described as a simple Regge pole) is exchanged we expect the universality of Pomeron parton distribution functions to apply. However, if the soft Pomeron pole is not the dominant exchange then we, a priori, have no good reason to expect the factorization of the x_P - and β -dependence (and even if factorization does hold there is no reason to expect universality of the extracted parton densities). Let us briefly explain how the Regge model leads to factorizable and universal Pomeron parton

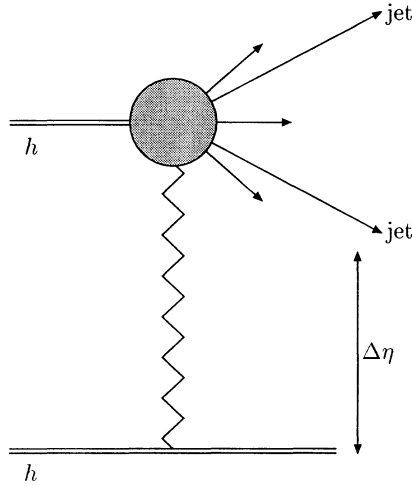


Fig. 7.7. Hard-diffractive production of jets in hadron-hadron diffractive scattering. The zig-zag line denotes the Pomeron exchange and $\Delta\eta$ denotes the final state rapidity gap.

distribution functions.

For the general diffractive process, $A + B \rightarrow A + X$, and assuming the Pomeron to be a simple Regge pole, we can write the diffractive cross-section as

$$M_X^2 \frac{d\sigma}{dt dM_X^2} = \frac{1}{16\pi} |\beta_A(t)|^2 \left(\frac{s}{M_X^2} \right)^{2\alpha_P(t)-2} \sigma_{BP}(M_X^2, t), \quad (7.57)$$

where $\beta_A(t)$ reflects the coupling of the Pomeron to the target, A , and σ_{BP} is the total cross-section for scattering particle B off the Pomeron.

In the case where the beam particle is a virtual photon, we probe the quark densities of the Pomeron, i.e. for scattering of transverse and longitudinal photons

$$\sigma_{\gamma P} \equiv \frac{4\pi^2\alpha}{Q^2} F_{T,L}^P(\beta, Q^2). \quad (7.58)$$

The Pomeron quark densities are defined by

$$F_2^P(\beta, Q^2) = F_L^P(\beta, Q^2) + F_T^P(\beta, Q^2) = \sum_i e_i^2 x f_{q/P}(\beta, Q^2).$$

These parton densities can also be probed in, for example, the hard-diffractive jet production process of Fig. 7.7 in which case we can write,

$$\frac{d\sigma(A + B \rightarrow A + jjX)}{dt dM_X^2 dp_T^2} = \frac{1}{16\pi} |\beta_A(t)|^2 \left(\frac{s}{M_X^2} \right)^{2\alpha_P(t)-2} \times \frac{d\sigma(BP \rightarrow jjX)}{dp_T^2}, \tag{7.59}$$

where

$$\frac{d\sigma(BP \rightarrow jjX)}{dp_T^2} = \sum_{i,j} \int dx_1 f_{i/B}(x_1, p_T^2) \int dx_2 f_{j/P}(x_2, p_T^2) \times \frac{d\hat{\sigma}(ij)}{dp_T^2}. \tag{7.60}$$

The sum is over all parton types, x_1 is the fraction of particle B 's momentum carried by parton i and x_2 is the fraction of the Pomeron momentum carried by parton j . The differential cross-section, $d\hat{\sigma}/dp_T^2$, is that of the hard sub-process, i.e. the scattering of partons i and j into the final state (producing a pair of partons with transverse momentum p_T relative to the collision axis) and is straightforward to compute in perturbative QCD.

Thus we see that Pomeron parton densities can be extracted from data on hard-diffractive processes just as proton parton densities can be extracted from hard non-diffractive scattering. In the case of the proton parton densities, one has the advantage of a momentum sum rule, which allows a constraint to be placed upon the size of the gluon density from a measurement of the quarks. It is far from clear that a similar sum rule holds for the Pomeron.

Of course the Pomeron is much more elusive than a hadron. Indeed, there is some ambiguity in using a single word to describe a wide range of phenomena. It remains to be seen whether the object which drives hard-diffractive jet production is the same as that which drives the rapidity gap processes in deep inelastic scattering and even whether the Regge inspired picture of the Pomeron as an effective target 'particle' is valid.

7.4 Summary

- Keeping the four-momentum transfer to the BFKL Pomeron

large is an excellent way to ensure the dominance of perturbative dynamics. The momentum transfer, $-t = \mathbf{q}^2$, acts as an effective infra-red cut-off. Contributions from Pomeron sizes larger than $\sim 1/q$ are heavily suppressed whilst the dominant contributions (from sizes $\gtrsim 1/q$) are characterized as a solution to the diffusion equation.

- In the target rest frame, the high energy scattering matrix is diagonalized by eigenstates of partonic configurations whose impact parameters are frozen over the time of the interaction. This facilitates an elegant physical picture of elastic scattering and diffraction dissociation processes.
- Despite the large virtuality, dissociation of virtual photons at high energies is dominated by non-perturbative physics. This is because the dominant configurations are of an aligned-jet nature.
- It may be useful to think of the photon dissociation process as one which performs deep inelastic scattering off a Pomeron target. For not too large diffracted masses, the Pomeron structure function for scattering off transverse photons can be approximated by $\sim \beta(1 - \beta)$, where β is the Bjorken- x of the Pomeron-photon system.